

Supplementary Information (SI)

Sulfur and Iron Co-doped Titanoniobate Nanosheets: a Novel Efficient Solid Acid Catalyst for Alcoholysis of Styrene Epoxide at Room Temperature

Lihong Zhang ^a, Chenhui Hu ^a, Junfeng Zhang ^a, Liyuan Cheng ^a, Zheng Zhai ^a, Jing Chen ^b, Weiping Ding ^a, Wenhua Hou ^a *

^a *Key Laboratory of Mesoscopic Chemistry of MOE, School of Chemistry and Chemical Engineering, Nanjing University, Nanjing 210093, P R China. E-mail: whou@nju.edu.cn. Fax: +86-25-83317761; Tel: +86-25-83686001.*

^b *Department of Applied Chemistry, College of Science, Nanjing University of Technology, Nanjing 210009, P R China.*

1 Experimental

1.1 Catalyst preparation

The layered potassium titanoniobate, KTiNbO_5 , was prepared by heating a stoichiometric mixture of K_2CO_3 , Nb_2O_5 and TiO_2 at $1100\text{ }^\circ\text{C}$ for 24 h. The corresponding protonic form, HTiNbO_5 , was obtained by reacting KTiNbO_5 with 6 M HNO_3 aqueous solution at room temperature for 3 days ^[1].

The $[\text{TiNbO}_5]^-$ nanosheets were prepared as follows: 1.0 g HTiNbO_5 was dispersed in 100 mL deionized water and then 10 % of TBAOH was added until the pH

reached 9~10. After reaction for 5 days, the supernatant solution containing $[\text{TiNbO}_5]^-$ nanosheets was collected by centrifugation. [2]

The nonmetal doping was carried out as follows: the obtained $[\text{TiNbO}_5]^-$ nanosheets were added with 1 mol/L HNO_3 to result in the immediate aggregation and then mixed with thiourea at a mass ratio of 1:2. The resulted mixture was heated in air at 400 °C for 2 h to obtain S-doped HTiNbO_5 nanosheets (noted as STN-400). For comparison, undoped HTiNbO_5 nanosheets (HTNNS) were also heated under the same conditions (noted as HTNNS-400).

The metal doping sample was prepared by using the ferric oxide hydrosol as iron source. The ferric oxide hydrosol was obtained by the forced hydrolysis method according to the literature with a little change³: Predetermined amounts of FeCl_3 (3 mol/L) and HCl (0.2 mol/L) were mixed at a volume ratio of 1:3 and then diluted to 300 mL by deionized water. The liquid mixture was then heated at 96 °C for 1 h and cooled to room temperature.

To prepare Fe-doped $[\text{TiNbO}_5]^-$ nanosheets (FTN), the ferric oxide hydrosol was slowly added to the above mentioned solution containing $[\text{TiNbO}_5]^-$ nanosheets under vigorous stirring. The flocculated product was centrifuged, washed thoroughly with distilled water and ethanol, and then dried at 60 °C.

To prepare S and Fe co-doped $[\text{TiNbO}_5]^-$ nanosheets (SFTN-400), 1.0 g FTN was finely milled with 2.0 g thiourea, and the resulted solid mixture was then heated in air at 400 °C for 2 h. For comparison, FTN itself alone was also directly calcinated at 400 °C for 2 h (FTN-400).

The whole preparation process is shown in Fig. S1.

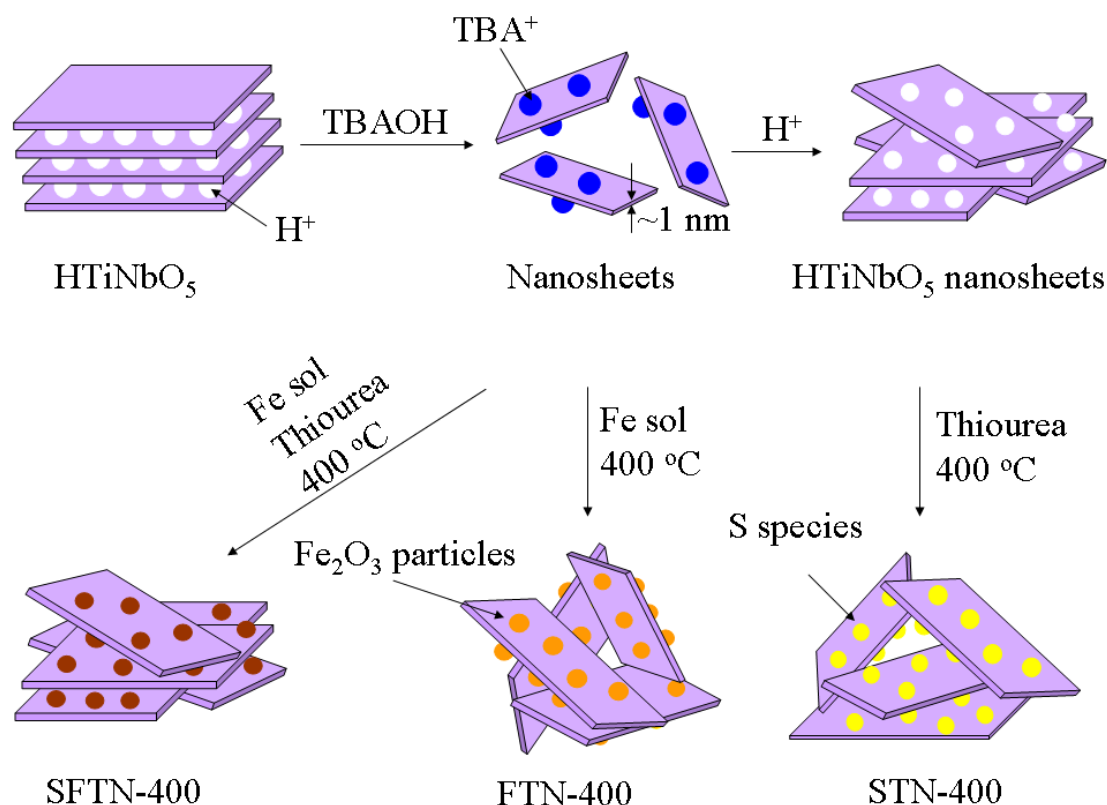


Fig. S1 Procedure for the formation of exfoliated and H⁺-restacking titanoniobate nanosheets and the corresponding S and Fe doping catalysts.

1.2 Catalyst test

In a typical alcoholysis reaction of styrene epoxide, 50 mg catalyst was added into a mixed solution of 1 mmol styrene epoxide and 2 mL of anhydrous alcohol (methanol, ethanol, propyl alcohol, isopropyl alcohol and butyl alcohol, respectively). The solution was stirred at room temperature to get the corresponding β -alkoxyalcohols. The reaction progress was monitored by gas chromatography (GC-122) and toluene (40 μ L) was used as the internal standard. Chromatographic conditions: injector temperature 230 °C; detector temperature 230 °C; column: a chiral β -cyclodextrin

capillary column (RESTEK RT-BetaDEXse, 30 m × 0.25 mm × 0.25 μm); temperature program: 60 °C for 1 min, 60–170 °C, 5 °C/min, 170 °C. Upon completion of the reaction, the catalyst was filtered off, washed thoroughly with corresponding alcohol, and finally calcinated with thiourea (mass ratio of 1:2) for reuse.

2 XRD analysis

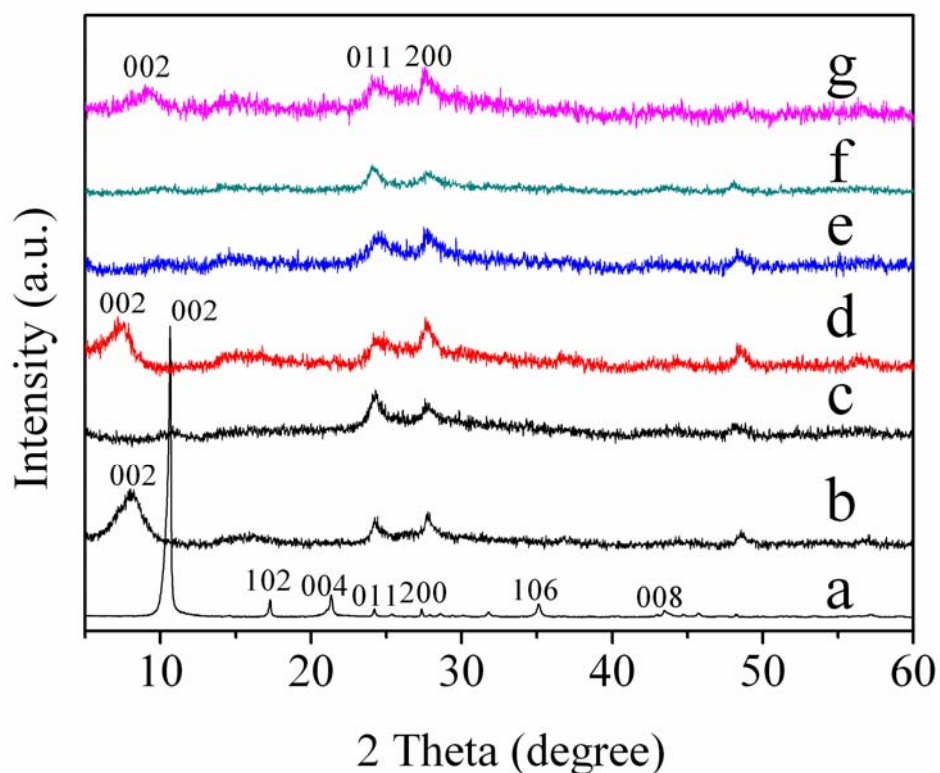


Fig. S2 XRD patterns of (a) HTiNbO₅, (b) HTNNS, (c) HTNNS-400 (d) FTN, (e) FTN-400, (f) STN-400 and (g) SFTN-400

The XRD patterns of the resulted catalysts are shown in Fig. S2. The as-prepared HTiNbO₅ exhibits a strong and sharp (002) reflection at $2\theta=10.6^\circ$, indicating a well-ordered lamellar structure with an interlayer distance of 0.83 nm. After exfoliation with TBAOH and flocculation with H⁺ ions, the (002) reflection of the resulted H⁺-restacking titanoniobate nanosheets became rather weak and shifted to a

lower angle (Fig. S2b), revealing a lower crystallinity and an irregular arrangement of nanosheets. In addition, after calcination in air at 400 °C, the characteristic (002) reflection fully disappeared (Fig. S2c), suggesting the relatively lower thermostability of HTNNS.

As shown in Fig. S2d, after the reaction of TBAOH-exfoliated $[\text{TiNbO}_5]^-$ nanosheets with ferric oxide hydrosol, the (002) diffraction peak of the resulted FTN is similar to that of HTNNS and the interlayer distance is increased to 1.17 nm, revealing the formation of a relatively disordered layered structure in which iron oxides were intercalated in the interlayers. After calcination at 400 °C, the resulted FTN-400 shows the complete absence of (002), indicating the collapse of a periodic layered structure. Similarly, S-doped sample STN-400 also shows no characteristic (002) diffraction peak of the layered structure.

However, when S and Fe were co-doped into $[\text{TiNbO}_5]^-$ nanosheets (SFTN-400), the characteristic (002) diffraction peak can be still observed at 9.0° . The corresponding interlayer distance is calculated to be 0.98 nm, which is larger than that of the original HTiNbO_5 . It indicates that the layered structure is still maintained after calcination at 400 °C and there is a synergetic effect between S and Fe species in the co-doped sample.

Meanwhile, all samples exhibit similar characteristic diffraction peaks corresponding to the $[\text{TiNbO}_5]^-$ layers of HTiNbO_5 at a 2θ range of $20\sim 30^\circ$, indicating that the basic structure of nanosheets is preserved.

3 Morphology analysis

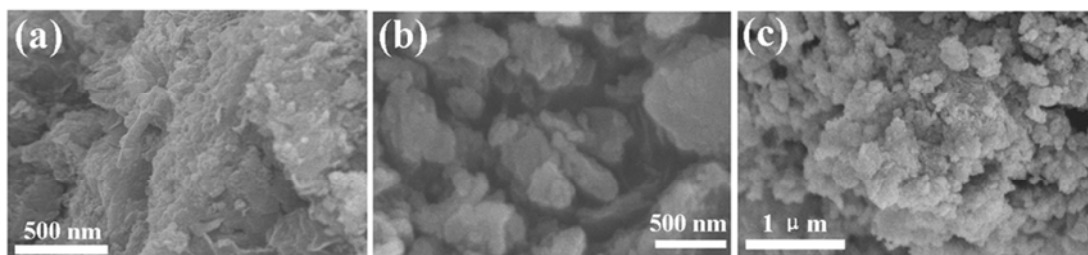
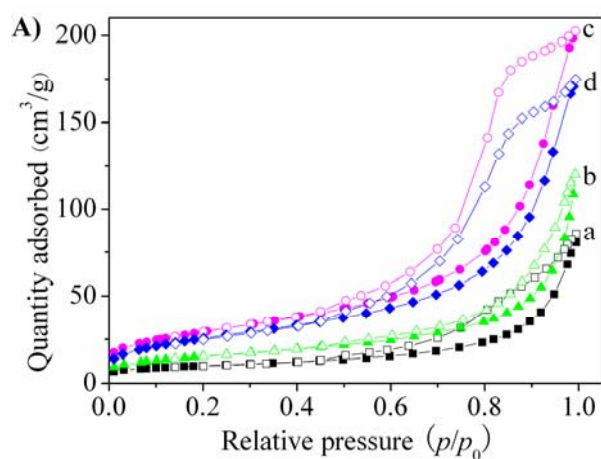


Fig. S3 SEM images of (a) HTNNS-400, (b) STN-400 and (c) FTN-400

After exfoliation and calcination, the resulted HTNNS-400 displays a rather loosely structure with a number of irregularly stacked nanosheets. Similarly, disorganized aggregates of small nanosheets are formed in STN-400 and FTN-400 and the ordered layered structure is no longer observed. It indicates that the layered structures of undoped, S-doped and Fe-doped titanoniobate nanosheets are not thermally stable up to 400 °C, being consistent with XRD results.

4 Surface area and porosity analysis



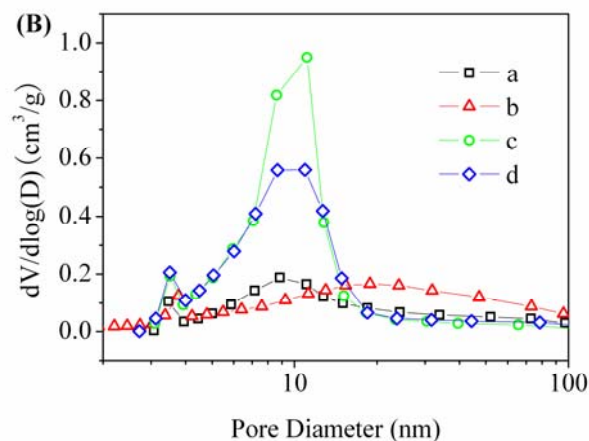


Fig. S4 (A) N₂ adsorption–desorption isotherms and (B) pore-size distribution curves of (a) HTNNS-400, (b) STN-400, (c) FTN-400 and (d) SFTN-400.

5 FT-IR spectra of adsorbed pyridine

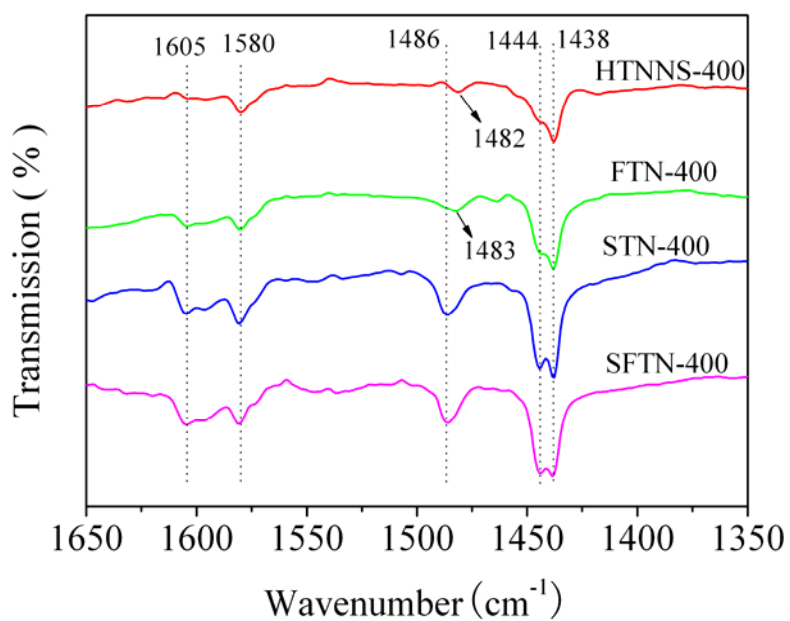


Fig. S5 FT-IR spectra of pyridine adsorbed on HTNNS-400, FTN-400, STN-400 and SFTN-400.

As shown in Fig. S5, all four catalysts exhibit IR bands at 1605, 1580, 1486, 1444 and 1438 cm⁻¹. These bands can be assigned to the pyridine coordinated to Lewis acid

sites⁴, revealing that the acid type of the resulted catalysts is mainly Lewis acid. In addition, compared with undoped catalyst HTNNS-400 and FTN-400, the characteristic band of Lewis acid at 1444 cm^{-1} in STN-400 and SFTN-400 becomes much sharper, indicating that the doping of S is more beneficial to the enhancement of the catalyst surface acidity than that of Fe.

6 XPS analysis

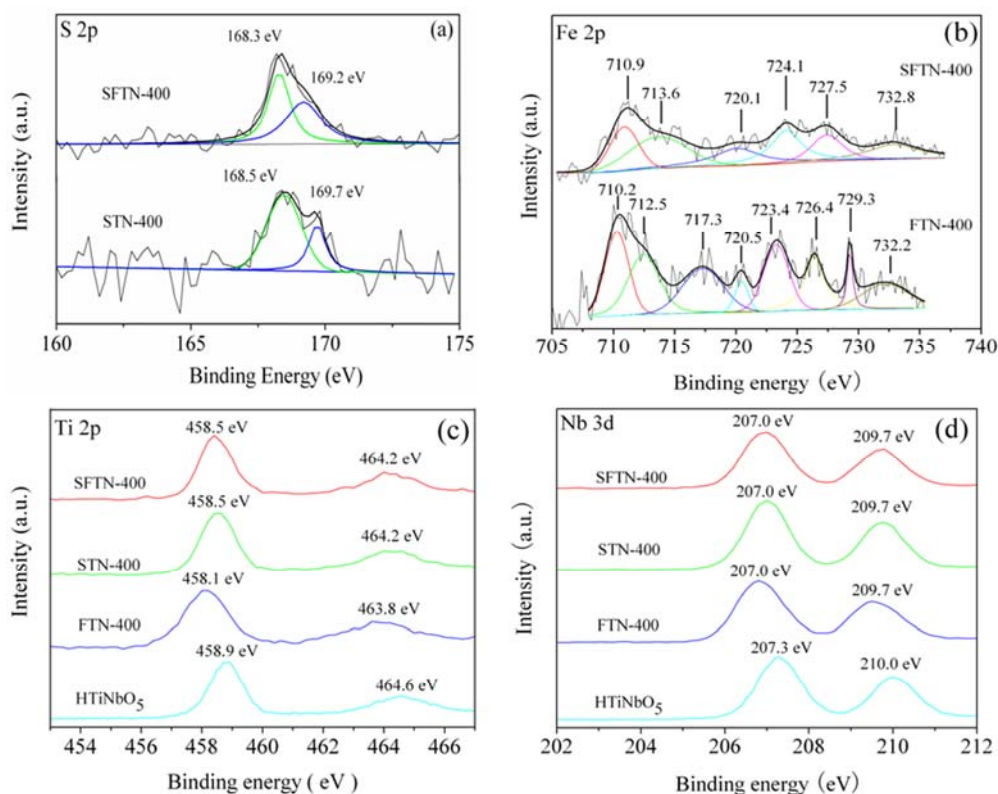


Fig. S6 XPS spectra of HTiNbO₅, FTN-400, STN-400 and SFTN-400.

XPS measurements were performed to determine the environment and chemical states of S, Fe, Ti and Nb in HTiNbO₅, STN-400, FTN-400 and SFTN-400. Fig. S6a displays S 2p XPS spectra of STN-400 and SFTN-400. There are two peaks around

168.5 and 169.7 eV for STN-400 sample, which could be assigned to the SO_4^{2-} ions.^[5] Compared with STN-400, the position of these two peaks is decreased respectively in SFTN-400 to about 168.3 and 169.2 eV. This result suggests that SO_4^{2-} ions in two catalysts are directly anchored on iron species and titanium niobate sheets respectively, based on the process of catalyst preparation. In addition, no signals were observed at 161-162 eV and 164 eV which can be ascribed to sulfide and elemental sulfur.^[6]

Fig. S6b shows Fe 2p XPS spectra of FTN-400 and SFTN-400. For FTN-400, the binding energy of Fe 2p_{3/2} can be decomposed into 710.2 and 712.5 eV, and that of Fe 2p_{1/2} fitted into 723.4 and 726.4 eV. And each peak is accompanied with a shake-up satellite in the ranges of 717–721 eV and 728–734 eV, respectively.^[7] From these values, it can be concluded that the surface iron species are trivalent and two different chemical environments of Fe^{3+} ions existed in FTN-400 arising from the presence of Fe-O-Ti and Fe-O-Ti(Nb).^[8, 9] By comparison, for SFTN-400, the binding energies of Fe 2p main peaks are increased by 0.7 eV and 1.1 eV respectively. Such a positive shift should be caused by the strong interaction between the iron and sulfate species, which may lead to stronger Lewis acid sites.

Ti 2p XPS spectra of FTN-400, STN-400, SFTN-400 and HTiNbO₅ are shown in Fig. S6c. Compared with HTiNbO₅, peaks of Ti 2p in FTN-400 are negatively shifted by 0.8 eV, implying the presence of Fe-O-Ti and Fe-O-Ti (Nb). After a further doping of S, the resulted SFTN-400 shows a decreased BE of Ti 2p only by 0.4 eV, being quite similar to the result obtained with STN-400. It indicates that SO_4^{2-} ions are tightly anchored on the surface of Fe species which ultimately gives rise to a much

lower outer electron density of Ti and then the BE of Ti 2p increase. Compared with HTiNbO₅, peaks of Nb 3d in three doped catalysts are negatively shifted by 0.3 eV, implying the presence of interaction between S or Fe and [TiNbO₅]- nanosheets.

7 IR analysis

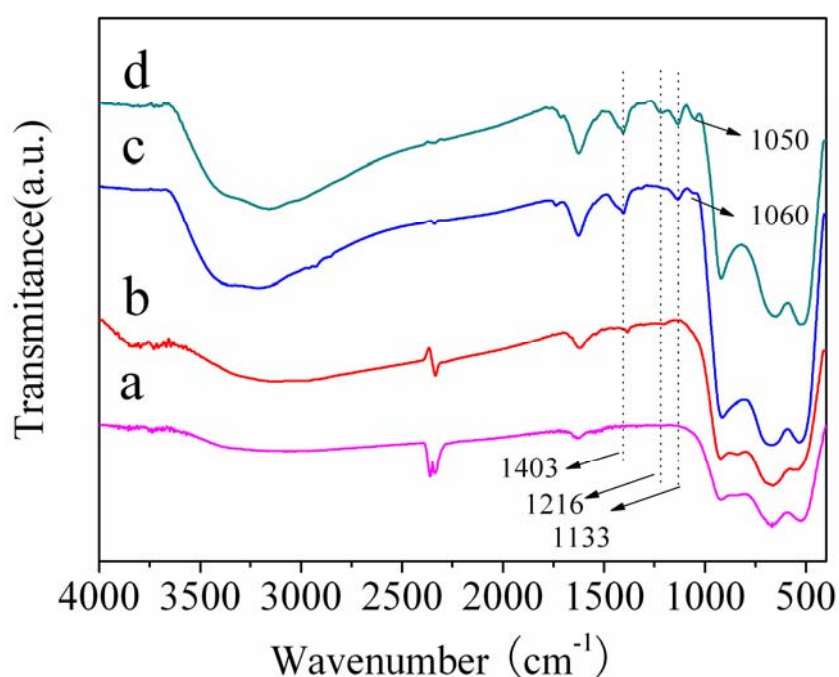


Fig. S7 FTIR spectra of (a) HTNNS-400, (b) FTN-400, (c) STN-400 and (d) SFTN-400.

The FTIR spectra of samples are shown in Fig. S7. For two S-doped samples, there are two peaks at 3500 – 3000 cm⁻¹ which can be attributed to the stretching vibration of free OH (3400 cm⁻¹) and the vibration of adsorbed water (3200 cm⁻¹), respectively, indicating the presence of hydroxyl groups on the surface of samples.^[10] The IR absorption bands in the range of 400-1000 cm⁻¹ are mainly arisen from vibrations of layered host.^[11] Compared with the undoped and Fe-doped samples, two S-doped

samples show new peaks in the region of 1400-1000 cm^{-1} . Concretely, the peak at 1403 cm^{-1} can be attributed to the stretching vibration of O=S=O.^[12] The absorption peaks at 1216 cm^{-1} and 1133 cm^{-1} can be attributed to the asymmetric and symmetric stretching vibrations of S=O, respectively, while the absorption peak at 1050 or 1060 cm^{-1} can be attributed to the asymmetric stretching vibration of S-O.^[12] For STN-400, the peaks at 1060 and 1133 cm^{-1} are characteristics of sulfate coordinated to metal in a bidentate model. But for SFTN-400, the adsorption peak of the asymmetric stretching vibration of S-O is shifted to a lower wavenumber at 1050 cm^{-1} and a new shoulder peak at 1216 cm^{-1} appears except 1133 cm^{-1} .^[12] This further suggests that sulfate was coordinated to different surface metals, and S-O-Fe and Fe-O-Ti (or Ti and Nb) bondings were formed in SFTN-400. In a word, the introduction of S results in the change of the surface structure of the corresponding catalysts.

Table S1 Some textural parameters of HTiNbO₅ and the corresponding derivatives

Sample	Interlayer distance (nm)	S _{BET} (m ² g ⁻¹)	Pore volume (cm ³ g ⁻¹)
HTiNbO ₅	0.83	3.7	-
HTNNS	1.06	41.7	0.131
FTN	1.17	73.1	0.210
HTNNS-400	-	35.0	0.133
FTN-400	-	106.0	0.315
STN-400	-	55.0	0.187
SFTN-400	0.98	94.0	0.272

References

- [1] W. H. Hou, J. Ma, Q. J. Yan and X. C. Fu, *J. Chem. Soc., Chem. Commun.*, 1993, 1144-1145.
- [2] A. Takagaki, M. Sugisawa, D. L. Lu, J. N. Kondo, M. Hara, K. Domen and S. Hayashi, *J. Am. Chem. Soc.*, 2003, 125, 5479-5485.

- [3] S. H. Kan, S. Yu, X. G. Peng, X. T. Zhang, D. M. Li, L. Z. Xiao, G. T. Zou and T. J. Li, *J. Colloid Interface Sci.*, 1996, 178, 673-680.
- [4] a) S. Valange, A. Beauchaud, J. Barrault, Z. Gabelica, M. Daturi and F. Canc, *J. Catal.*, 2007, 251, 113-122; b) H. A. Prescott, Z. J. Li, E. Kemnitz, A. Trunschke, J. Deutsch, H. Lieske and A. Auroux, *J. Catal.*, 2005, 234, 119-130.
- [5] G. Colón, M. C. Hidalgo, G. Munuera, I. Ferino, M. G. Cutrufello and J. A. Navío, *Appl. Catal. B: Environ.*, 2006, 63, 45-59.
- [6] L. K., A. Ghorbel, P. Grange and F. Figueras, *Appl. Catal. B: Environ.*, 2005, 59, 105-111.
- [7] H. Qi, C. Qian and J. Liu, *Nano Lett.*, 2007, 7, 2417-2421.
- [8] J. Faye, A. Bayle, M. Trentesaux, S. Royera, F. Dumeignil, D. Duprez, S. Valange and J. M. Tatibouet, *Appl. Catal. B: Environ.*, 2012, 126, 134-143.
- [9] R. S. Prakasham, G. S. Devi, K. R. Laxmi and C. S. Rao, *J. Phys. Chem. C*, 2007, 111, 3842-3847.
- [10] J. L. Roper-Vega, A. Aldana-Perez, R. Gomez, M.E. Nino-Gomez, *Appl. Catal. A: Gen.*, 2010, 379, 24-29.
- [11] X. J. Guo, W. H. Hou, G. L. Bao, Q. J. Yan, *Solid State Ionics*, 2006, 177, 1293-1297.
- [12] (a) J. L. Roper-Vega, A. Aldana-Pérez, R. Gómez, M. E. Niño-Gómez, *Applied Catalysis A: General*, 2010, 379, 24-29; (b) C. Han, M. Pelaez, V. Likodimos, A. G. Kontos, P. Falaras, K. O'Shea, D. D. Dionysiou, *Applied Catalysis B: Environmental*, 2011, 107, 77-87; (d) L. K. Noda, R. M. de Almeida, L. F. D.

Probst, N. S. Goncalves, *Journal of Molecular Catalysis A: Chemical*, 2005, 225, 39-46; (e) D. J. Guo, X. P. Qiu, L. Q. Chen, W. T. Zhu, *Carbon*, 2009, 47, 1680-1685; (f) Y. X. Niu, M. Y. Xing, J. L. Zhang, B. Z. Tian, *Catal. Today*, 2013, 201, 159-166.